

Fig.1 COL13 RNA accumulates to high levels in hypocotyl. (a) Quantitative real time-PCR analysis of *AtCOL13* transcript abundance in different tissues. R=Root, S=Stem, L=Leaf, SAM=Shoot apical meristem, H=Hypocotyl, F=Flower. (b) Activity of *COL13* promoter revealed by β -glucuronidase (GUS) staining in Arabidopsis seedlings. Bar=100 mm.

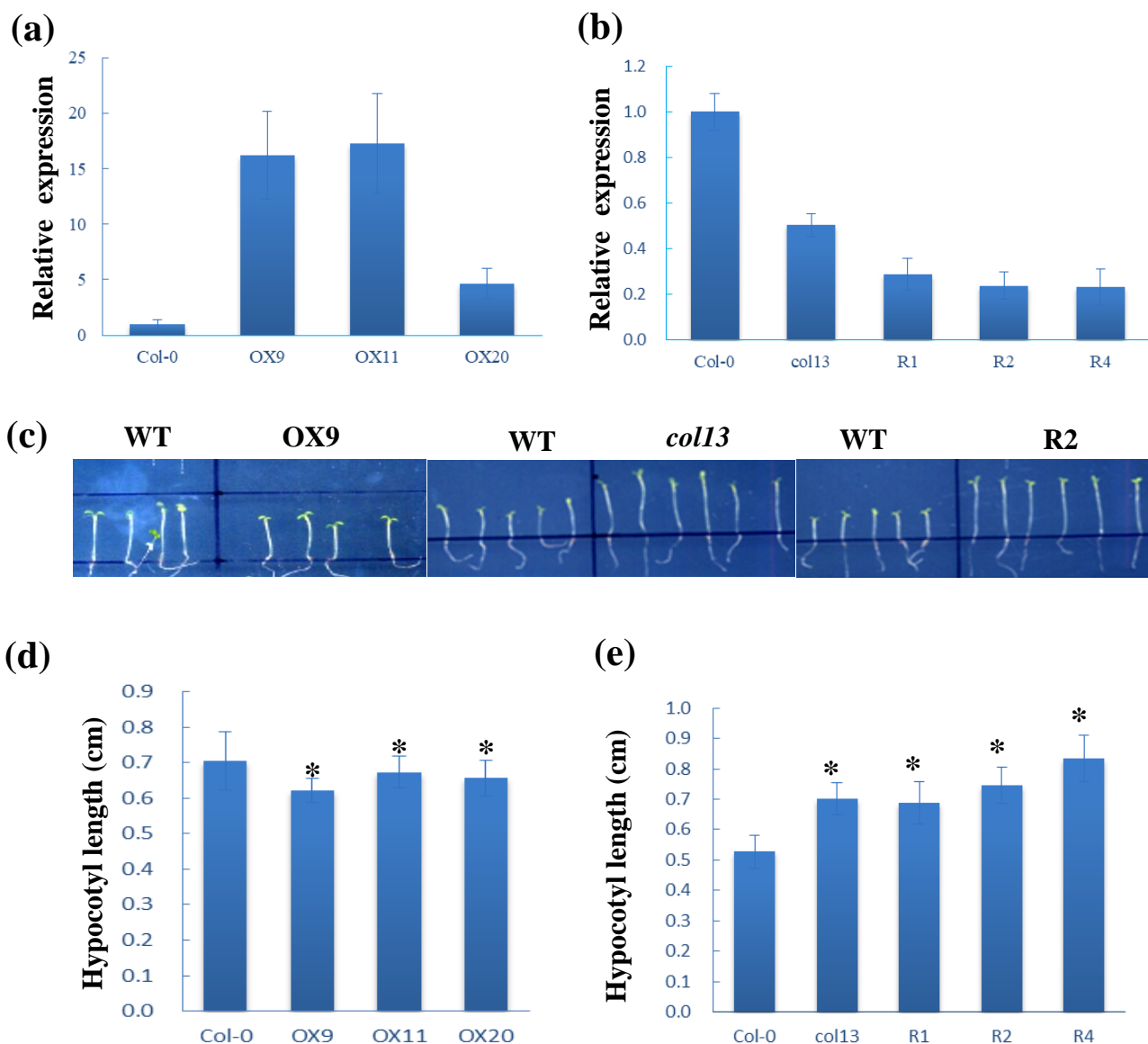


Fig.2 COL13 regulates hypocotyl elongation under red-light conditions. (a) Relative expression of *COL13* in Col-0 and overexpression (OX) lines. (b) Relative expression of *COL13* in Col-0, T-DNA mutant (*col13*) and RNAi lines (R1-1 etc.). (c)-(e) Phenotypic analysis seedlings of the indicated genotypes were grown in the presence of red light. Images of representative seedlings are shown in (c). The hypocotyl lengths of the indicated genotypes were measured at the 5th or 3rd day, and are shown in (d) and (e), respectively. Error bars indicate SD (n > 15). Asterisks indicate that hypocotyl lengths in OX9 and *col13*, *COL13* RNAi are significantly different with WT under red light (P < 0.05).

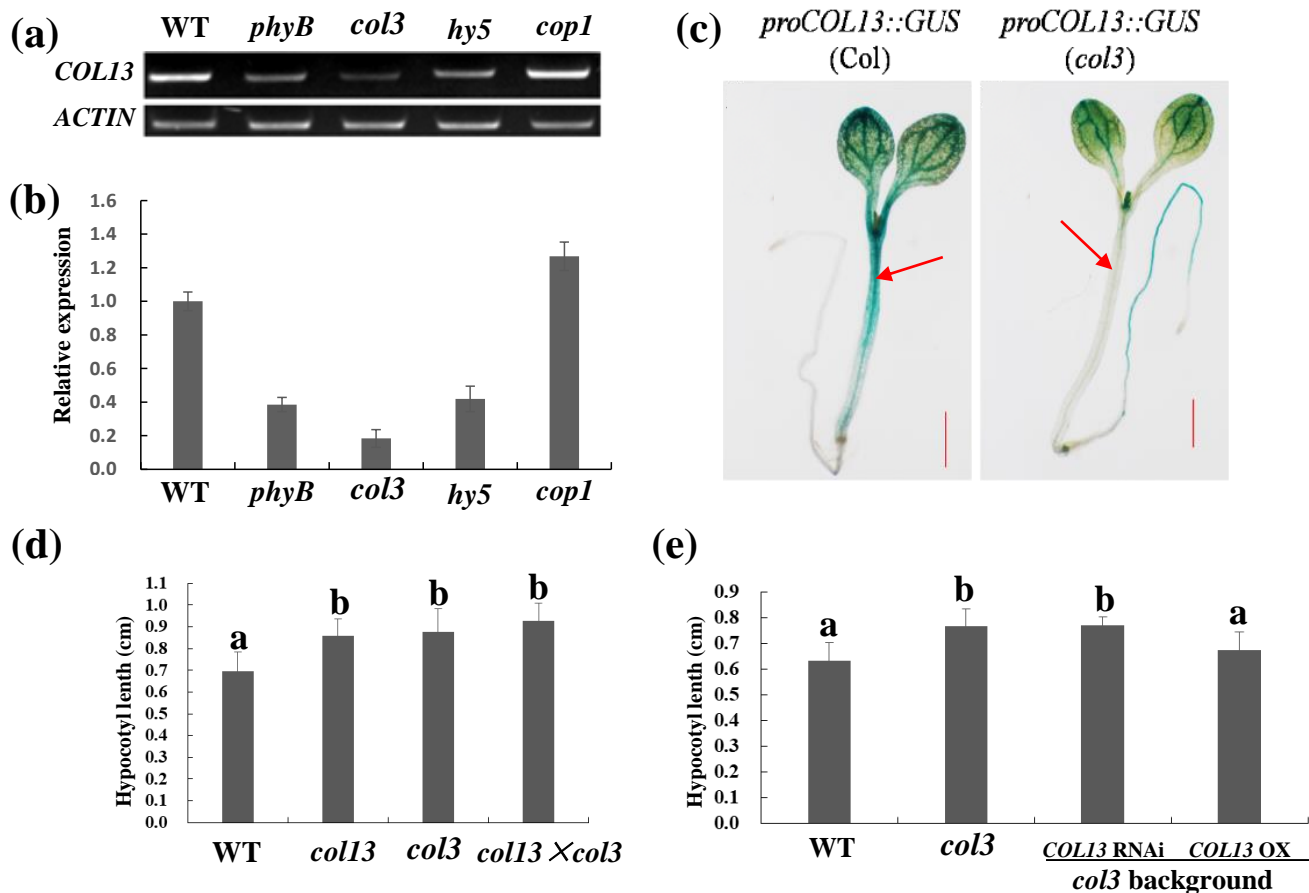
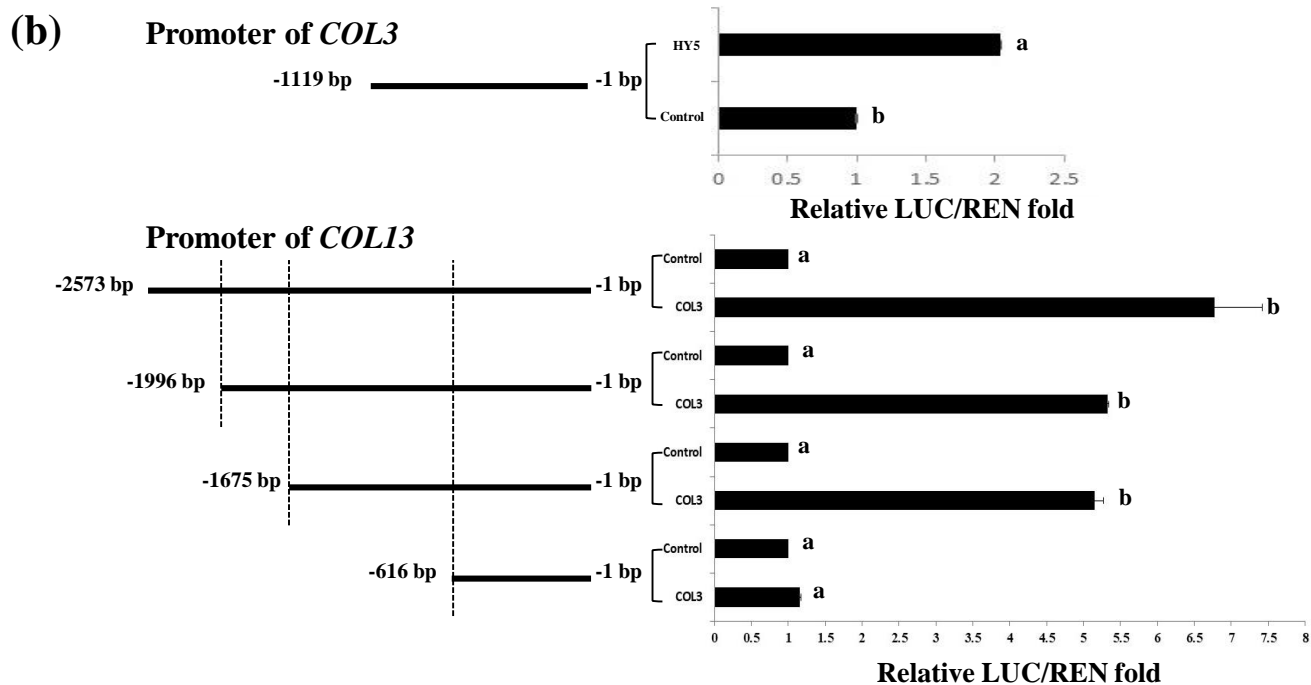
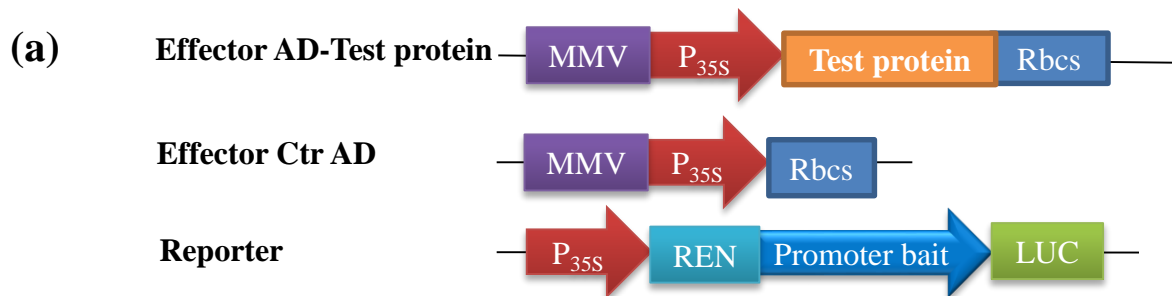


Fig. 3 Genetic interaction and physiological characterization of hypocotyl elongation. (a) Semi-quantitative RT-PCR analyses of *COL13* expression in *phyB*, *col3*, *hy5* and *cop1* mutants. (b) qRT-PCR analyses of *COL13* expression in *phyB*, *col3*, *hy5* and *cop1* mutants. (c) Activity of the *COL13* promoter revealed by β -glucuronidase (GUS) staining in WT and *col3* mutant backgrounds. (d) Hypocotyl length in WT, single- and double-mutant plants. Here we use the F1 hybrid of Col-0 × WS as WT. (e) Hypocotyl length in WT and *col3* plants compared to transgenic plants with *COL13* RNAi or *COL13* overexpression (OX) in the *col3* background. Here we use WS as WT. Error bars indicate SD ($n > 15$). Lower-case letters indicate significantly different data groups (hypocotyl length) of the indicated seedlings grown in red light.



(c)

COL3-HA	-	+	+	+	+	+
Biotin-P	+	+	+	+	+	+
Competitor	-	-	1X	5X	10X	25X

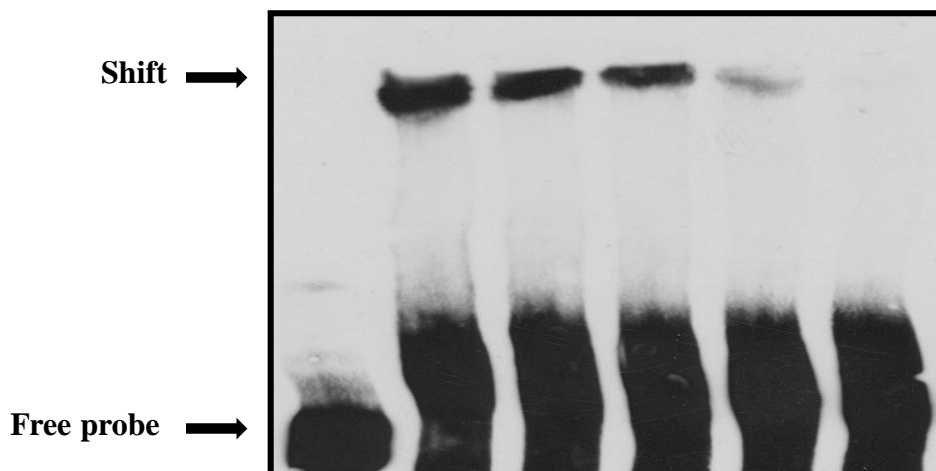


Fig.4 Analysis of the binding of HY5 to *COL3* promoter, and *COL3* to *COL13* promoter truncations. (a) Diagram of constructs used. The AD-HY5 or AD-COL3 fusion gene driven by the 35S promoter produces a potential effector protein, while the AD protein alone represents a negative control for basal activity of *COL3* promoter or each *COL13* promoter truncation. The *LUC* gene driven by the series of *COL3* promoter or *COL13* promoter truncations tests the ability of the AD-HY5 or AD-COL3 fusion protein to bind to each promoter truncation. (b) The fusion protein AD-HY5, but not AD alone, can effect *LUC* expression from the *COL3* promoter truncations, and the fusion protein AD-COL3, but not AD alone, can effect *LUC* expression from some of the *COL13* promoter truncations. (c) Electrophoretic mobility shift assay (EMSA) analysis showing the binding of COL3 to the -1675 bp and -616 bp promoter of *COL13* in vitro. The black arrow indicates binding of COL3 to the biotin-labeled *COL13* promoter. The + and – represent the presence and absence of corresponding components, respectively. Competition experiments were carried out by adding 5-, 10- and 25-fold excessive competitor.

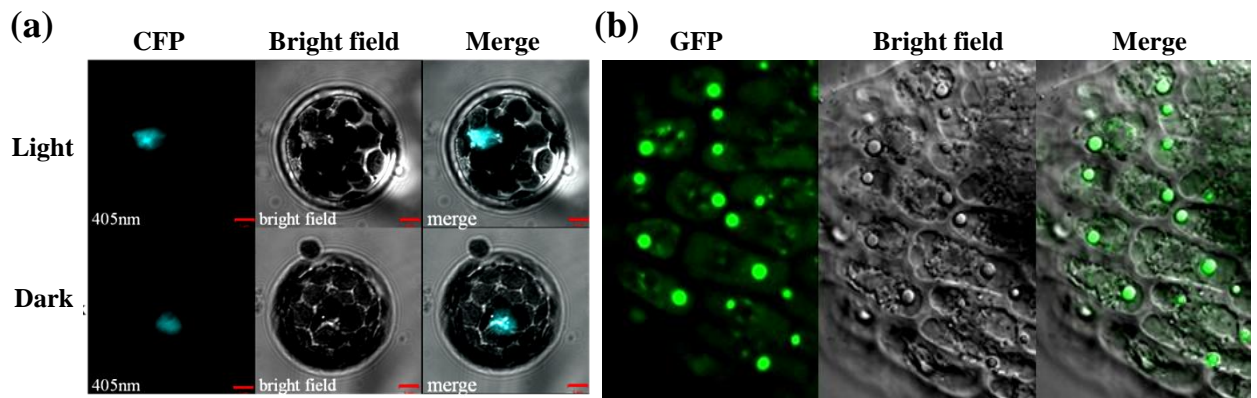


Fig.5 Subcellular localization of COL13. (a) COL13-CFP localizes to the nucleus in protoplasts. (d) COL13-GFP localizes to the nucleus in root tip cells.

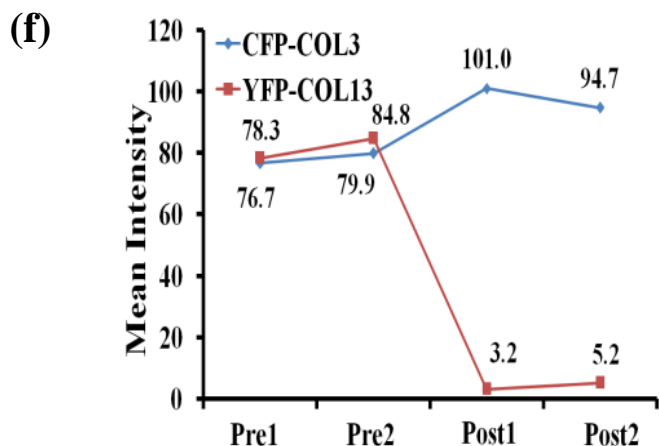
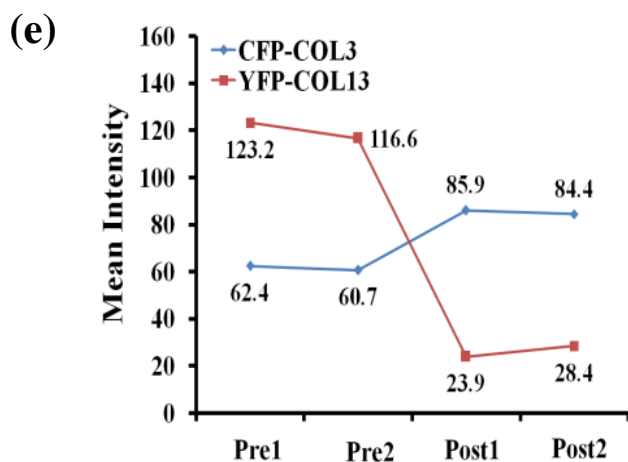
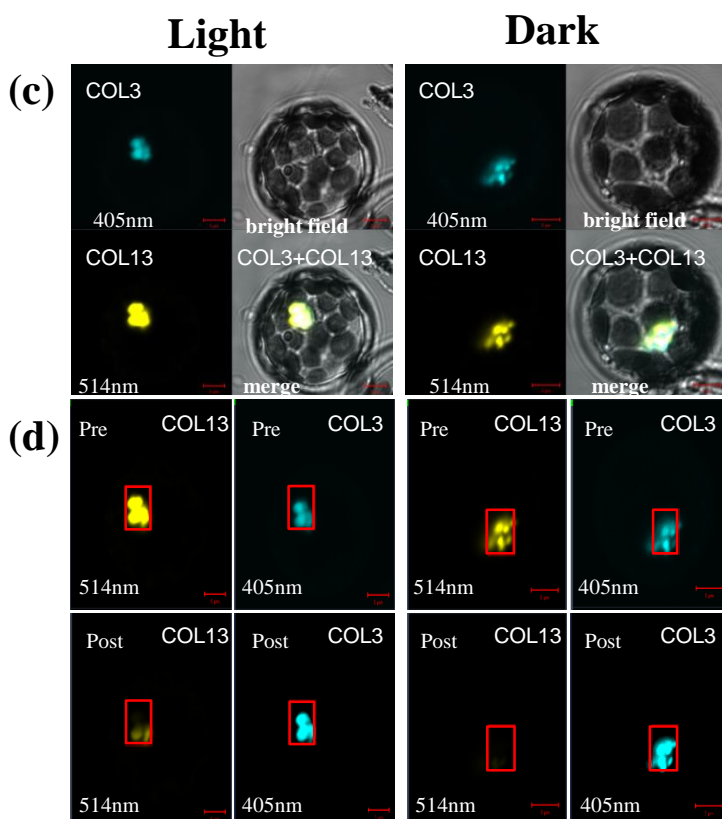
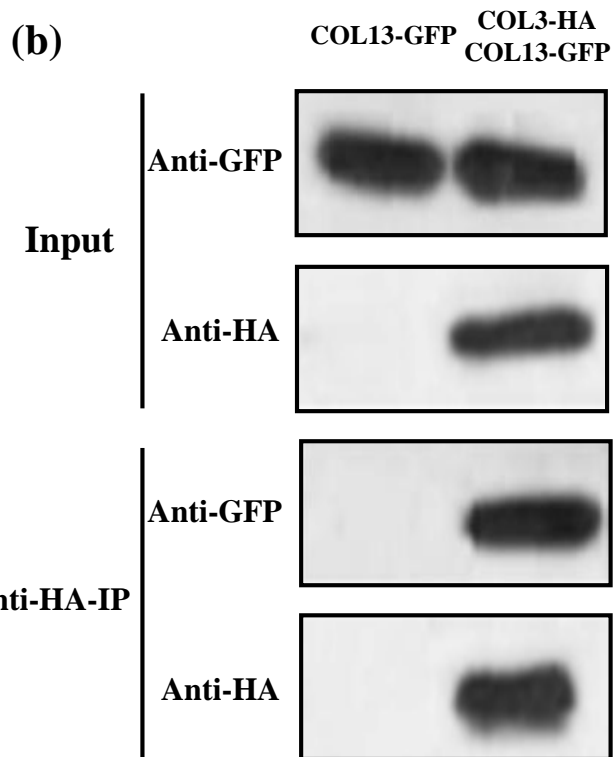
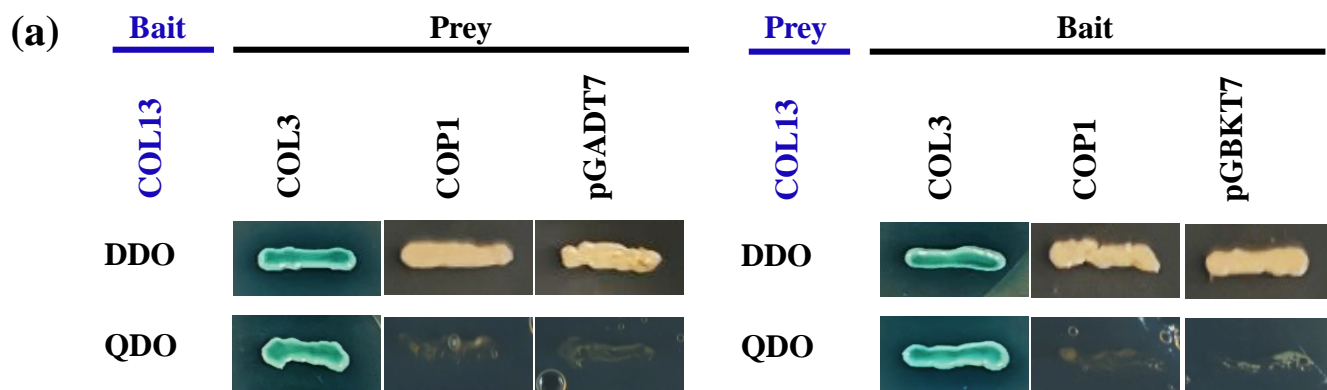
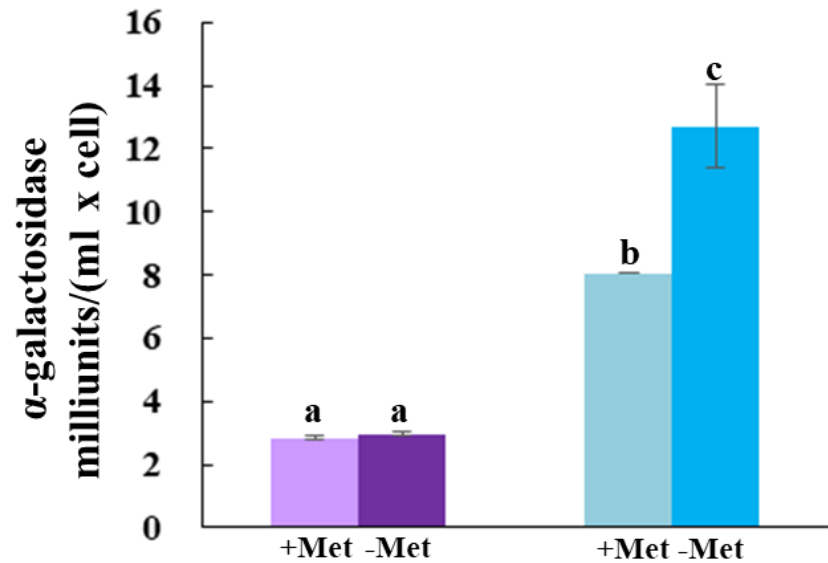


Fig.6 COL13 interacts with COL3. (a) Yeast Two-Hybrid assay between COL13 and COL3. DDO, Double Dropout; QDO, Quadruple Dropout; pGADT7, prey plasmid; pGBKT7, bait plasmid. (b) Co-immunoprecipitation (Co-IP) in *Arabidopsis*. Immunoprecipitations (IPs) were performed on protein extracted from 10-d-old *Arabidopsis* seedlings grown under long-day illumination (16L: 8D) at 22°C. Leaf tissues were harvested 1 h after the light cycle commenced. IP was performed using anti-HA antibody and COL13 was co-immunoprecipitated with anti-GFP antibody. A 5% input was used. Western blots were performed on 10% (wt/vol) precast gels (Bio-Rad). (c) COL3-CFP and COL13-YFP colocalize to the nucleus in protoplasts in light and dark. (d-f) FRET between CFP-COL3 and YFP-COL13 analyzed by acceptor bleaching in the nucleus. The top panels in (d) show a representative pre-bleach nucleus coexpressing YFP-COL13 and CFP-COL3 excited with either a 514- or a 405-nm laser in light and dark, resulting in emission from YFP (yellow) or CFP (blue), respectively. The bottom panels in (d) show the same nucleus post-bleaching after excitation with a 514- or a 405-nm laser. The relative intensities of both YFP and CFP were measured before and after bleaching, as indicated in (e) and (f).

(a)



pGADT7	+	-
pGADT7-COP1	-	+
COL3-COL13-pBridge	+	+

(b)

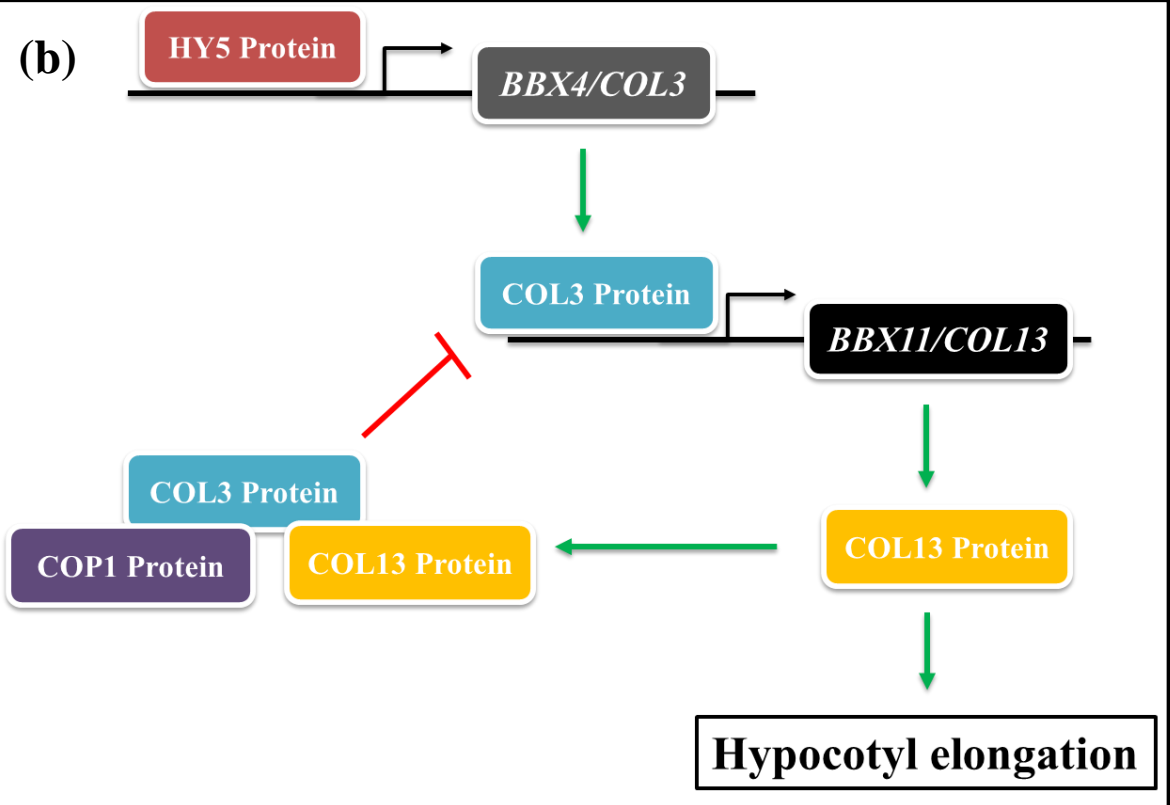


Fig.7 COL13 promotes the interaction between COL3 and COP1. (a) Yeast three-hybrid analysis of the COP1-COL3 interaction in the presence of COL13. Normalized Miller Units were calculated as a ratio of α -galactosidase activity in yeast. Additionally, normalized Miller Units here are reported separately for yeast grown on media without or with 1 mM methionine (Met), corresponding to induction (-Met) or repression (+Met) of *Met25* promoter-driven *COL13* expression, respectively. Means and SEM for three biological repetitions are shown. Lower-case letters indicate significant difference of α -galactosidase. (b) A model representing the HY5-COL3-COL13 regulatory chain and COP1-dependent COL3-COL13 feedback pathway in regulation of hypocotyl elongation.